

Use of EMI Response Coefficients from Spheroidal Excitation and Scattering Modes to Classify Objects via SVM

Beijia Zhang^a, Kevin O'Neill^{bc}, Tomasz M. Grzegorzczak^a, Jin Au Kong^a

^aMassachusetts Institute of Technology, 77 Massachusetts Avenue, Cambridge, MA, USA 02139

^bThayer School of Engineering, Dartmouth College, Hanover, NH, USA 03755;

^cEngineer Research and Development Center Cold Regions Research and Engineering Laboratory, 72 Lyme Road, Hanover, NH, USA 03755

ABSTRACT

Electromagnetic induction (EMI) has been shown to be a promising technique for unexploded ordnance (UXO) detection and discrimination. The excitation and response of a UXO or any other object to EMI sensors can be described in terms of scalar spheroidal modes consisting of associated Legendre functions. The spheroidal response coefficients B_k^j correspond to the k^{th} spheroidal response to the j^{th} spheroidal excitation. The B_k^j have been shown to be unique properties of an object, in that objects producing different scattered fields must be characterized by different B_k^j . Therefore, the B_k^j coefficients may be useful in discrimination. We use these coefficients rather than dipole moments because they are part of a physically complete, rigorous model of the object's response. Prolate spheroidal coordinate systems recommend themselves because they conform most readily to the proportions of objects of interest.

In clearing terrain contaminated by UXO, the ability to distinguish larger buried metallic objects from smaller ones is essential. Here, a Support Vector Machine (SVM) is trained to sort objects into different size classes, based on the B_k^j . The classified objects include homogeneous spheroids and composite metallic assemblages. Training a SVM requires many cases. Therefore, an analytical model is used to generate the necessary data. In simulation studies, the SVM is very successful in classifying independent sets of objects of the same type as the training set. Furthermore, we see that the B_k^j are not related to size or signal strength of the object in any simple or visually discernible way. However, SVM is still able to sort the objects correctly. Ultimately, the success of the SVM trained with synthetic (model derived) data will be evaluated in application to data from a limited population of real objects, including UXO.

Keywords: UXO, spheroidal modes, EMI, quasistatic, SVM, induction, inversion, discrimination, ordnance

1. INTRODUCTION

1.1. Motivation

Clean up of UXO sites is expensive due to high false alarm rates. The high false alarm rates are due in part to the presence of clutter at these sites. EMI sensing is used to detect buried objects, and UXO discrimination is based on the EMI response of the objects.

1.2. UXO discrimination and classification

One of the most basic types of discrimination is determining whether a buried object is a UXO or a piece of clutter. To do such discrimination, it is necessary to ask what characteristics distinguish clutter objects from UXO. To this effect, we have determined four key points:

1. Elongation: Objects are considered elongated when the length along one dimension of the object is at least twice the length of the dimension along the transverse direction of that object. Many UXO are intended to be launched into the air and thus have an elongated, prolate spheroidal shape. In general, clutter objects do not adhere to this principle.

2. Body of Revolution (BOR): UXO are almost always a BOR. Even the presence of fins or other small deviations on a UXO does not affect the response of the object to the extent that we are able to distinguish it from true BOR objects when classification of such objects is concerned.¹ Clutter can be any random shape and thus has no higher likelihood to be BOR.
3. Size: Though some small UXO types exist, the majority of UXO are large. Therefore large objects are of great interest to workers who clean up UXO sites. Small clutter particles can have a strong EMI response if they are buried at shallow depths which is often the case. Since the strength of the object's response is such a poor indication of the object's size, discrimination processing is necessary to avoid the costly task of digging up these clutter objects.
4. Homogeneity: UXO are usually composed of many different materials while clutter is often homogenous. The ability to distinguish between homogeneous and heterogeneous objects is another tool in being able to discriminate clutter objects from UXO.

In previous work, the ability to distinguish elongated from non-elongated objects has been investigated.¹ Our current work focuses on classifying objects by size, homogeneity, and BOR properties.

1.3. Spheroidal mode background

The magnetic field generated by the transmitter is called the primary magnetic field, $H^{PR}(\bar{r})$. The secondary magnetic field, $H^S(\bar{r})$, is the response of the target. In the EMI regime of a few Hz to a few 100 kHz, these magnetic fields can be considered irrotational if the target is embedded in a non-conducting medium. Therefore, the primary and secondary magnetic field can be given in terms of the gradient of a scalar potential: $\Psi_j^{PR}(\bar{r})$ for the primary potential and $\Psi_k^S(\bar{r})$ for the secondary potential. Furthermore, these two potentials can be expressed as a linear superposition of a finite number of modes each of which is a solution to Laplace's equation. The spheroidal coordinate system was selected as the basis for this decomposition.

$$U^{PR}(\bar{r}) = \frac{d}{2} \sum_{m=0}^{\infty} \sum_{n=m}^{\infty} \sum_{p=0}^1 b_{pmn} P_n^m(\eta) P_n^m(\xi) T_{pm}(\phi) \quad (1)$$

$$U^{PR}(\bar{r}) = \frac{d}{2} \sum_j b_j \Psi_j^{PR}(\bar{r}) \quad (2)$$

$$U^S(\bar{r}) = \frac{d}{2} \sum_{m=0}^{\infty} \sum_{n=m}^{\infty} \sum_{p=0}^1 B_{pmn} P_n^m(\eta) Q_n^m(\xi) T_{pm}(\phi) \quad (3)$$

$$U^S(\bar{r}) = \frac{d}{2} \sum_k B_k \Psi_k^S(\bar{r}) \quad (4)$$

$$T_{pm}(\phi) = \begin{cases} \cos(m\phi), & p = 0 \\ \sin(m\phi), & p = 1 \end{cases}$$

In equations 1 to 4, $P_n^m(\)$ and $Q_n^m(\)$ are the associated Legendre functions of the first and second kind, respectively. Equation 2 is a compact way of writing equation 1. Likewise, equation 4 is a compact way of writing equation 3. Each j or k mode index is a compact form to write all the indices of the Legendre functions for each mode and can be expanded into the form $j = (p,m,n)$ and $k = (p,m,n)$. Unlike the spherical coordinate system, the spheroidal coordinate system must be uniquely specified with an interfocal distance d.

The primary and secondary magnetic fields that can be obtained by taking the gradient of equations 2 and 4, respectively.

$$\bar{H}^{PR}(\bar{r}) = \frac{-d}{2} \sum_j b_j \nabla \Psi_j^{PR}(\bar{r}) \quad (5)$$

$$\bar{H}^S(\bar{r}) = \frac{-d}{2} \sum_k B_k \nabla \Psi_k^S(\bar{r}) \quad (6)$$

$$\bar{H}^S(\bar{r}) = \sum_j b_j \bar{H}_j^S(\bar{r}) = \sum_j b_j \frac{-d}{2} \sum_k B_k^j \nabla \Psi_k^S(\bar{r}) \quad (7)$$

\bar{H}_j^S represents the secondary field response to a single excitation mode j . We can decompose \bar{H}_j^S in the same manner as equation 6 to obtain the B_k^j coefficients in equation 7. These coefficients correspond to the k^{th} mode of the spheroidal response to the j^{th} mode of the spheroidal excitation. It can be mathematically proven that all objects with unique EMI responses also have unique B_k^j coefficients.^{5,13} We take advantage of the uniqueness property of these coefficients in our discrimination work and inverse problem solutions.

1.4. SVM background

Determining if an object is clutter or an UXO by using the B_k^j coefficients of the object is a pattern classification recognition problem. SVM is a supervised statistical learning algorithm.²⁰ The basic idea of SVM is that all data points can be mapped into an n -dimensional space where each dimension corresponds to each “ n ” input parameter or characteristic of that data point. Therefore in our research, each scatterer is considered as a data point and the B_k^j of each object become the dimensions for the n -dimensional space. Parameters of that scatterer, such as size or elongation form the classification categories.

By processing a collection of “training data” for which we already know the class of each object, an SVM becomes aware of where the objects of each class are positioned in the n -dimensional space. Then the basic objective of an SVM is to find the optimal hyperplane that correctly separates the points of the two classes as completely as possible. This process is called “training the SVM.” When a new object of an unknown class is presented to SVM, SVM only has find on which side of the hyperplane the new object falls to decide which class it belongs to. Therefore, once a SVM is trained, the classification process is normally very fast. A quantitative performance measure of a trained SVM is determined by the accuracy with which it classifies a set of “test data,” generated independently of the training data. The actual class for each test data object is known but not given to the SVM. The result of the SVM classification on the test data is then compared to the true class to determine the error rate.

Most data points in their native space are not usually directly separable with a hyperplane. Therefore the SVM will non-linearly map the n -dimensional input space into a higher dimensional feature space using a kernel function. In this higher dimensional feature space, the data can usually be separated.²⁰

2. METHODOLOGY

2.1. mySVM

We chose to use a prepackaged implementation of SVM called mySVM which has been shown to be successful in past classification work.¹ The software mySVM was developed at the University of Dortmund and is an implementation of SVM introduced by Vapnik.²⁰ This software is freely distributed on the Internet.²¹ We used mySVM in its “pattern matching” mode with a radial kernel function.

2.2. Forward model

It would be extremely difficult to take measurements from enough unique objects to obtain the necessary amount of training data. Therefore, we use a forward model for homogeneous spheroids and composite objects to generate objects

with arbitrary permeability, conductivity, and size.^{5,6,11} With a forward model, we can create an infinite amount of training data.

2.2.1. Necessity of a fast forward model

SVM requires a large set of training data. In our experience, optimal results were obtained when over 2000 unique training objects were used. Therefore any forward model used must be relatively fast. Though a large portion of this preliminary study focuses on synthetic data and objects, training on synthetic random objects will always be necessary even when we want to classify objects using real field measurements. It is not cost effective or efficient to find and measure enough real objects to form a large and effective training data set. Past classification studies have incorporated the B_k^j from measurements of some real objects into the training set.¹ However, the majority of the training data was always synthetic.

2.2.2. Spheroidal model

For the initial investigation, we can model scatterers in two general ways. First, the simplest way is to model a single spheroid. Algorithms have been developed to generate the spheroidal B_k^j coefficients and the vectorial H fields for any arbitrary spheroid in terms of size and elongation, i.e. interfocal distance, with variable permeability and conductivity.^{5,6,11} In this model, spheroids can be used to represent objects ranging from flat disks to long thin rods. From the calculated H fields, we can solve for the appropriate B_k^j coefficients to mimic the procedure that would need to take place for actual measured data.

It is necessary to note that although modeling a spheroid in a spheroidal coordinate system with the same interfocal distance may seem to be a natural fit, this is not an appropriate approach when classification is the primary goal. Rather, we must fix all coordinate systems at a single universal interfocal distance and solve for the B_k^j of all objects within this single coordinate system. Comparing B_k^j of different objects is the crux of our SVM classification work, but this comparison is meaningless unless the coefficients are from the exact same spheroidal coordinate system.

Secondly, we can create composite, heterogeneous objects with two small spheroids that are coaxial and are separated by a distance of 1mm as show in in Figure 1. Thus this composite object is a BOR object. The two spheroids that form this composite object are given different permeability and conductivity values. The H-field response of each spheroid was calculated and summed. The B_k^j were then solved for that total H-field. We assume no interaction between the two spheroids. Experimentation has shown that this is a reasonable assumption when one object of two closely spaced objects is not permeable.

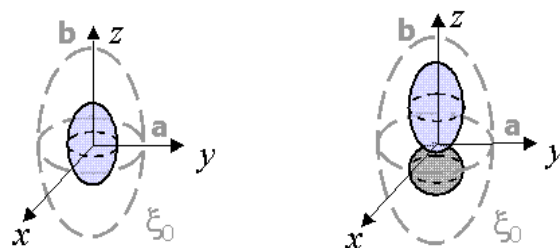


Fig. 1. The SVM was trained using single spheroids (left) or composite objects (right). Note that the interfocal distance for the coordinate system must be the same across all training and test objects.

2.2.3. Selection of B_{jk} modes

The GEM-3 sensor manufactured by Geophex is a commonly used EMI sensor. It essentially consists of two concentric wire loops with a current running in opposite directions on each. The H-field in the center of the loops is null so

measurements of the secondary field are taken at this center point. As with any sensor, the GEM-3 produces fields which can be expressed as an infinite linear combination of orthogonal primary modes. However, the GEM-3 primary fields are dominated by a few modes while the other modes are negligible. It has been found that four to seven modes are sufficient to describe the primary potentials.¹ The four most dominant modes are $j = (0,0,1)$, $(0,0,2)$, $(0,1,1)$, and $(1,1,1)$ and are called the “basic primary modes.” Modes $(0,0,3)$, $(0,1,2)$, and $(1,1,2)$ are also significant but are not as dominant as the basic primary modes. We will call the combination of all seven modes, “extended primary modes.”

The secondary fields are strongly dependent on the properties of a scattering object. Therefore, we are unable to determine a priori which secondary modes will be most dominant. We do know, however, that when the observation is far from the scatterer, the dipole model provides a good approximation to the object. Mode $k = (0,1,1)$ corresponds to the dipole component in the x direction, $(1,1,1)$ corresponds to the y direction, and $(0,0,1)$ corresponds to the z direction. So we choose to truncate the secondary modes, retaining those that have m and n less than or equal to 1. Therefore with 7 modes for j and 4 modes for k , we have a total of 28 B_k^j coefficients. We consider the response of the objects at two different frequencies: one high at 10950 Hz and one low at 210 Hz. Furthermore, the real and imaginary components of each fundamental mode are considered as independent inputs to the SVM. Therefore we have a total of 112 input parameters for SVM.

2.3. Previous work

Applying SVM to the problem of classifying spheroids based on elongation has already been shown to be successful.¹ In previous work, the B_k^j of 394 materially homogeneous spheroids of various elongations were used to train SVM. For test data, 93 independent spheroids were generated with the forward model and classified by the SVM as elongated ($e > 2$) or not. Of those 93, only 3 were incorrectly classified.

3. CLASSIFICATION BASED ON OBJECT SIZE

In this study, we are interested in classifying objects based on size. Since our synthetic objects are up to 0.08 cubic meters in volume, we identify objects with volumes greater than 0.04 cubic meters as “large.” Objects with volumes smaller than 0.04 cubic meters are considered “small.” This chosen threshold and range of object sizes are completely arbitrary, and a properly trained SVM can identify objects for any desired threshold.

3.1. Single spheroid

3.1.1. Method

Our initial investigation focused on single spheroid objects. We used training data comprised of 2000 synthetic objects. 1000 were “small” objects and 1000 were “large” objects. The single spheroid training set and single spheroid test set consisted of objects that either had relative permeability of 100 and a conductivity of 2×10^6 S/m or was non-permeable and had a conductivity of 2×10^7 S/m. The size of each object was randomly assigned and ranged from 0.001 m^3 to 0.08 m^3 . The elongation was also randomly assigned and ranged from 0.1 to 4 (ratio of major axis to minor axis length). The interfocal distance of our coordinate system was 1.22 and was the universal standard for the generation of all synthetic objects in our study. Generation of the B_k^j for all 2000 synthetic objects took roughly 24 hours on a 3GHz Pentium 4 PC. Training the SVM took only a few minutes.

3.1.2. Results

The test data consisted of 200 single spheroid objects, with 100 large objects and 100 small objects. Each object had a random elongation, random size, and one of the two possible material compositions that were used in the generation of the training data. Shown in Figure 2 is a scatter plot that summarizes the SVM classification of these test data. Each point represents one single test object. The vertical axis is the actual volume of each object. The horizontal axis is the sum of the squares of the B_k^j input parameters for each object. Triangular data points represent objects that SVM

predicted as large. Circle data points represent objects that SVM predicted as small. Table 1 is the corresponding confusion matrix. For this classification, there are 4 erroneously classified objects so we consider the error to be 2%. As expected from a properly functioning SVM, all the erroneously classified objects are close to the boundary.

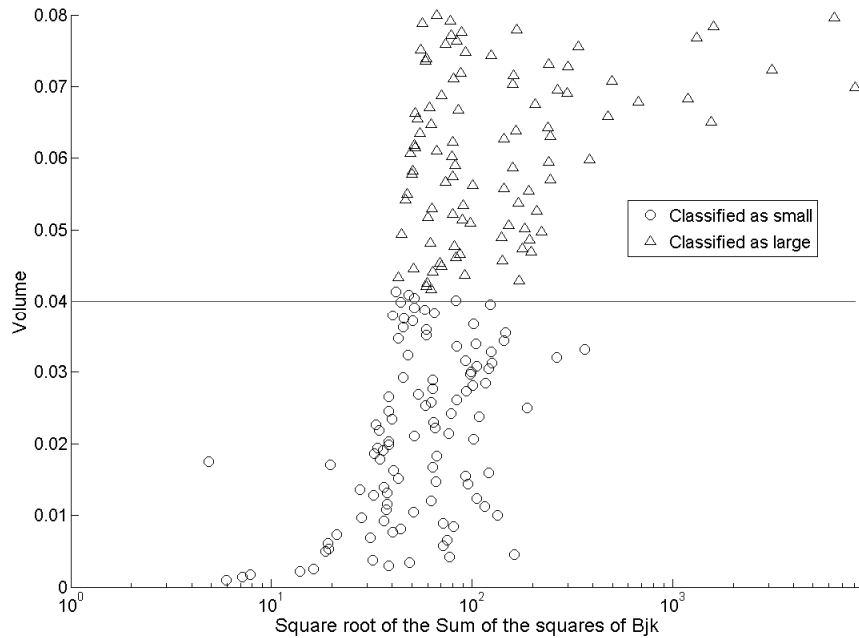


Fig. 2. The result of classification of single spheroids by a SVM trained on single spheroids. Triangles represent objects that were classified as large; circles represent objects classified as small. The vertical location of each marker is determined by the actual size of the corresponding object. The horizontal location is determined by the overall magnitude of the secondary spheroidal coefficients. Horizontal line indicates the boundary between “large” and “small” objects.

Table. 1. Corresponding confusion matrix for Figure 2.

		Predicted	
		Large	Small
Actual	Large	96	4
	Small	0	100

One very important feature of Figure 1 is that the size of the object has no obvious relationship with the magnitudes of the B_k^j coefficients. One might simply assume that larger objects simply have larger overall B_k^j coefficients and that application of SVM is unnecessary to do classification. If that were the case, then all data points in Figure 1 should be distributed close to a diagonal pattern in the previous figure. This pattern does not appear yet SVM is quite successful in classifying objects by size. Therefore, there is a hidden, underlying pattern makes it necessary to use SVM to do classification.

3.2. Composite spheroids

3.2.1. Method

The second type of object that we are interested in is heterogeneous objects. This type of object is a composite of two different arbitrarily sized spheroids. One spheroid has a relative permeability of 100 and a conductivity of 2×10^6 S/m. The other spheroid is non-permeable and has a conductivity of 2×10^7 S/m. As with the single spheroid case, the elongation and size of each spheroid is randomly assigned and the total volume of both objects ranged from 0.001 m^3 to 0.08 m^3 . 2000 training cases and 200 test cases were used for the composite object cases.

3.2.2. Summary of results

Table 2 summarizes the accuracy of SVM classification for single spheroid objects and composite spheroid objects. As detailed earlier, when SVM is trained on single objects, it only gives a 2% error when classifying single objects. When this trained SVM is used to classify composite objects, it can give an error of 12%. Likewise, when an SVM is trained using composite objects and then tested using composite objects, it gives an error of 2.5%. When this SVM is tested using single objects, it produces an error of 8.0%. We feel that the errors rates of 8.0% and 12.0% for when the SVM is tested with different types of objects from those it was trained with indicate that there is some underlying pattern of the B_k^i that can identify whether an object is large or small. Furthermore, if we anticipate both single and composite type objects to be present, we can also train the SVM with both single and composite objects as was done to generate the third column of Table 2. Here this SVM is capable of classifying both types of objects with only a small loss of accuracy yet a high gain of generality.

Table 2. Percent error for volume based classification of the single spheroid test set and the composite spheroid test set. The three columns indicate three different SVM that formed using different sets of training data: single spheroids alone, composite spheroids alone, and both single and composite spheroids together.

	Training Data		
	Single	Composite	Composite and Single
Test Data Single	2.0%	8.0%	4.0%
Test Data Composite	12%	2.5%	3.5%

3.3. Classification based on volume with added noise

3.3.1. Method

Since the measurements collected in the field are subject to both instrument and environmental noise, our understanding of SVM classification limitations would be incomplete without examining SVM classification of noisy signals. It would be unnatural and incorrect to simply add noise to the B_k^i . Noise added this way does not replicate how one would expect to receive noisy field data. We must therefore add noise to the H vectorial fields calculated from the B_k^i . The H fields were calculated for a grid of points that is 12 points by 12 points with a 6m span and with two elevations

separated by 20cm. We added -10dB and -3dB Gaussian noise to the calculated H fields. Noise is calculated with respect to the mean over space of each vectorial H component of each object. We then solved for the B_k^i of that noisy magnetic field using a point matching method. We used Gaussian noise because noise from the sensor and environment, barring large pieces of clutter, tends to be Gaussian. -3dB of noise is within the reasonable range of expected noise in measured data.

3.3.2. Results

Shown in Table 3 is a summary of the percent errors that arise when two types of trained SVM classify single spheroids whose B_k^i were derived from their magnetic field signals that have added noise. SVM is trained on either clean synthetic data alone or an equal part mixture of clean and noisy synthetic data. When SVM is trained only on clean data, it does very well when classifying test objects that are uncorrupted by noise. However, it is unable to generalize for noisy data. The two instances of 50% error in the table were created because this trained SVM classified all noise corrupted objects as large. When the SVM is trained on some noisy data along with clean data, it becomes much more robust. This trained SVM is able to classify both clean and noisy data with a relatively good level of accuracy. The three groups of test data and two groups of training data shown in Table 3 were all generated randomly and independently from each other.

Table 3. Percent error for volume based classification of the single spheroid test set and the composite spheroid test set. The three columns indicate three different SVM that formed using different sets of training data: single spheroids alone, composite spheroids alone, and both single and composite spheroids together.

	Training Data	
	Single Object (Clean)	Single Object (Clean and Noisy with -10dB noise)
Test Single Objects (Clean)	2.0%	7.0%
Test Single Objects (with -10dB noise)	50%	12%
Test Single Objects (with -3dB noise)	50%	30%

4. CLASSIFICATION BASED ON THE HOMOGENEITY OR HETEROGENEITY OF AN OBJECT'S COMPOSITION

4.1. Method

As mentioned, one of the overall goals of this project is to develop the ability to distinguish between UXO and clutter objects. Since clutter pieces tend to be materially homogeneous while UXO tend to be heterogeneous, we trained our SVM to distinguish between homogeneous objects made up of two spheroids with the same material properties and heterogeneous composite objects where the two spheroids have different material properties. The two possibilities in material composition for the spheroids are, again, a relative permeability of 100 and a conductivity of 2×10^6 S/m or non-permeable and a conductivity of 2×10^7 S/m. Homogeneous objects are randomly assigned one of those possibilities. Size and elongation, again, are randomly assigned. We train with 2000 objects; half are homogeneous and half are heterogeneous.

4.2. Results

Shown in Table 4 is the confusion matrix when the trained SVM classifies a 400 member test data set. This test data set was generated in the same manner as but independently of the training data set. We note that the error of 14.75% in this classification scheme is higher than when the SVM classifies objects based on size. However, we expect improvements to be made in our ability to classify on the basis of the heterogeneity of the objects. Presently we are unable to explain why the SVM classification is skewed toward classifying objects as heterogeneous.

Table 4. Confusion matrix for classification of heterogeneous versus homogeneous composite spheroidal objects.

		Predicted	
		Homog.	Heterog.
Actual	Homog.	142	58
	Heterog.	1	199

5. CLASSIFICATION BASED ON BOR LIKENESS

5.1. Method

We also noted that many UXO tend to be BOR while the same cannot be said of clutter. Therefore we attempted to classify objects as BOR or non-BOR. Shown in Figure 3 are two types of composite objects, each consisting of two materially different spheroids. If their rotational axes lie on the same line as before, the composite object is BOR. If their axes are merely parallel, then the object is non-BOR. We use a 2000 member training data set. Half of that set are BOR; half are non-BOR.

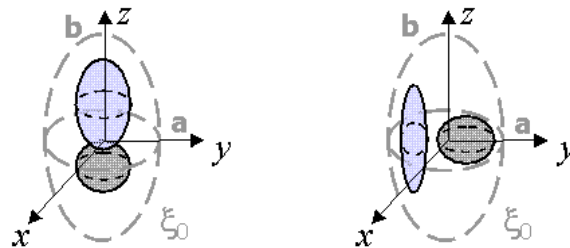


Fig. 3. Two types of composite objects: BOR and non-BOR. Both objects are materially heterogeneous.

5.2. Results

With a test set of 200 composite spheroidal objects, we are able to achieve perfect classification when we classified objects as BOR or non-BOR. This was expected since previous work concerning the application of spheroidal modes to UXO work has shown that BOR objects consistently have zero value coefficients for certain secondary modes.¹ Unlike

the patterns that SVM is able to extract when classifying on the basis of homogeneity or size, the pattern here is much more obvious.

Table. 5. Confusion matrix for classification of heterogeneous versus homogeneous objects.

		Predicted	
		BOR	Non-BOR
Actual	BOR	100	0
	Non-BOR	0	100

6. CONCLUSION

We have achieved moderately accurate to very accurate classification of objects based on volume, heterogeneity, and BOR likeness. For classification based on size, we have shown that correct classification is achievable for both single objects and composite objects. Our SVM can be trained so that it can learn to generalize for both single and composite objects. Furthermore, we are able to do relatively good volume classification for objects that have substantial noise added to their H field signals by training the SVM with noisy data.

7. FUTURE WORK

We are in the process of examining the effect of noise in other aspects of our classification work besides classification based on volume. Furthermore we are extending our collection of test and training objects to include more non-BOR objects. Creating a more robust SVM for noisy data is also an ongoing project for us in all aspects of our classification research. We hope to eventually create a decision tree--based on the four key characteristics that distinguish UXO from clutter objects--that will determine if an object is a UXO or not. We recently have started working with a new forward model for heterogeneous BOR objects of random shape and size. We anticipate that this will permit even more accuracy and robustness for our SVM. It is worth mentioning that although this paper concentrated on using spheroids or objects composed of spheroids, the spheroidal mode coefficients can describe any arbitrary object. The use of the spheroidal coordinate system was chosen since it is a convenient coordinate system. UXO objects tend to have a somewhat spheroidal shape so their response can be described without needing to use too many modes. Use of spheroidal mode coefficients does not mean that the modeled objects must be spheroids.

Finally, we have begun the foundation work toward applying our SVM to measurements from real objects.

REFERENCES

1. X. Chen, *Inverse Problems in Electromagnetics*, PhD thesis, Massachusetts Institute of Technology, May 2005.
2. X. Chen, K. O'Neill, B. E. Barrowes, T. M. Grzegorzcyk, and J. A. Kong, "Application of a spheroidal-mode approach and a differential evolution algorithm for inversion of magneto-quasistatic data in UXO discrimination," *Inverse Problem*, vol. 20, pp. S27–40, December 2004.
3. B. E. Barrowes, K. O'Neill, T. M. Grzegorzcyk, X. Chen, and J. A. Kong, "Broadband electromagnetic induction solution for a conducting and permeable spheroid," *IEEE Trans. on Geoscience and Remote Sensing*, vol. 42, pp. 2479–2489, November 2004.

4. B. E. Barrowes, Kevin O'Neill, Tomasz M. Grzegorzczak, Jin Au Kong, "On the asymptotic expansion of the spheroidal wave function and its eigenvalues for complex size parameter", *Studies in Applied Mathematics*, vol. 113, nr. 3, page(s) 271-301, October 2004.
5. B. E. Barrowes, *Electromagnetic Scattering and Induction Models for Spheroidal Geometries*. PhD thesis, Massachusetts Institute of Technology, January 2004.
6. C. D. Moss, *Numerical Methods for Electromagnetic Wave Propagation and Scattering in Complex Media*, PhD thesis, Massachusetts Institute of Technology, January 2004.
7. B. E. Barrowes, T. M. Grzegorzczak, J. A. Kong, and K. O'Neill, "Broadband Analytical Solution of the Electromagnetic Induction (EMI) Response by Spheroidal Objects Under Arbitrary Excitation", *Progress in Electromagnetic Research Symposium (PIERS)*, page(s) 127, 13-16 October, Honolulu, Hawaii, 2003.
8. X. Chen, K. O'Neill, T. Grzegorzczak, B. Barrowes, C. Moss, B.-I. Wu, and J. A. Kong, "Fundamental mode approach in electromagnetic induction scattering and inversion," in *Progress in Electromagnetic Research Symposium (PIERS)*, page(s) 318, 13-15 October, Honolulu, Hawaii, 2003.
9. C. D. Moss, Tomasz M. Grzegorzczak, J. A. Kong, and K. O'Neill, "A Hybrid Time Domain Solution of Electromagnetic Induction Scattering from Axisymmetric Objects", *Progress in Electromagnetic Research Symposium (PIERS)*, page(s) 308, 13-16 October, Honolulu, Hawaii, 2003.
10. C. D. Moss, K. O'Neill, T. M. Grzegorzczak, and J. A. Kong, "A Hybrid Time Domain Method To Calculate Electromagnetic Induction Scattering From Targets with Arbitrary Skin Depths", *The 19th Annual Review of Progress in Applied Computational Electromagnetics (ACES)*, page(s) 390-396, 24-28 March, Monterey, CA, 2003.
11. C. O. Ao, *Electromagnetic Wave Scattering by Discrete Random Media with Remote Sensing Application*. PhD thesis, Massachusetts Institute of Technology, June 2001.
12. C. O. Ao, H. Braunisch, K. O'Neill, J. A. Kong, L. Tsang, and J. T. Johnson, "Broadband electromagnetic induction response from conducting and permeable spheroids," *Proc. SPIE*, vol. 4394: *Detection and Remediation Technologies for Mines and Minelike Targets VI*, Orlando, April 16-20, 2001.
13. H. Braunisch, *Methods in Wave Propagation and Scattering*, Ph.D. thesis, Massachusetts Institute of Technology, Feb. 2001.
14. H. Braunisch, C. O. Ao, K. O'Neill, and J. A. Kong, "Magnetoquasistatic response of a distribution of small conducting and permeable objects," in *Proc. IEEE Int. Geosci. Remote Sensing Symp. (IGARSS)*, Honolulu, July 24-28, 2000, vol. 4, pp. 1424-1426.
15. K. Sun, K. O'Neill, L. Liu, F. Shubitidze, I. Shamatava, K. D. Paulsen, "Analytical solutions for EMI scattering from general spheroids with application in signal inversion for UXO discrimination," *Proceeding of SPIE, Detection and Remediation Technologies for Mines and Minelike Targets VIII*, Orlando, Florida, 21-25 April 2003, 1035-1045.
16. F. Shubitidze, K. O'Neill, K. Sun, I. Shamatava, and K.D. Paulsen, "A Hybrid Full MAS and combined MAS/TSA algorithm for electromagnetic induction sensing," *ACES (Applied Computational Electromagnetics Society) Journal*, special issue on ACES 2003 Conference Part II, vol. 19, No. 1b, March 2004, pp112-126.
17. F. Shubitidze, K. O'Neill, I. Shamatava, K. Sun and K.D. Paulsen, "Analysis of EMI scattering to support UXO discrimination: heterogeneous and multiple objects," *Proceeding of SPIE, Detection and Remediation Technologies for Mines and Minelike Targets VIII (or48)*, Orlando, Florida, 21-25 April 2003, pp928-939.
18. J. R. Wait. *Electromagnetic Wave Theory*. Harper and Row, 1985.
19. J. R. Wait "A Conducting Permeable Sphere in the Presence of a Coil Carrying an Oscillating Current" *Canadian Journal of Physics*, vol. 21, 1953.
20. V. Vapnik, *Statistical Learning Theory*, Wiley, 1998.
21. S. Rüping, *mySVM-Manual*, University of Dortmund, Lehrstuhl Informatik 8, 2000, <http://www-ai.cs.uni-dortmund.de/SOFTWARE/MYSVM/index.html>